Supplementary data

Catalytic properties of free-base porphyrin modified graphite electrodes for electrochemical water splitting in alkaline medium

Bogdan-Ovidiu Taranu[1], Eugenia Fagadar-Cosma[2,*]

[1]National Institute for Research and Development in Electrochemistry and Condensed Matter,
Dr. A. Paunescu Podeanu Street, No. 144, 300569 Timisoara, Romania
[2]Institute of Chemistry "Coriolan Dragulescu", Mihai Viteazu Ave. 24, 300223 Timisoara, Romania

*corresponding author: efagadar@yahoo.com or efagadarcosma@acad-icht.tm.edu.ro

Scheme

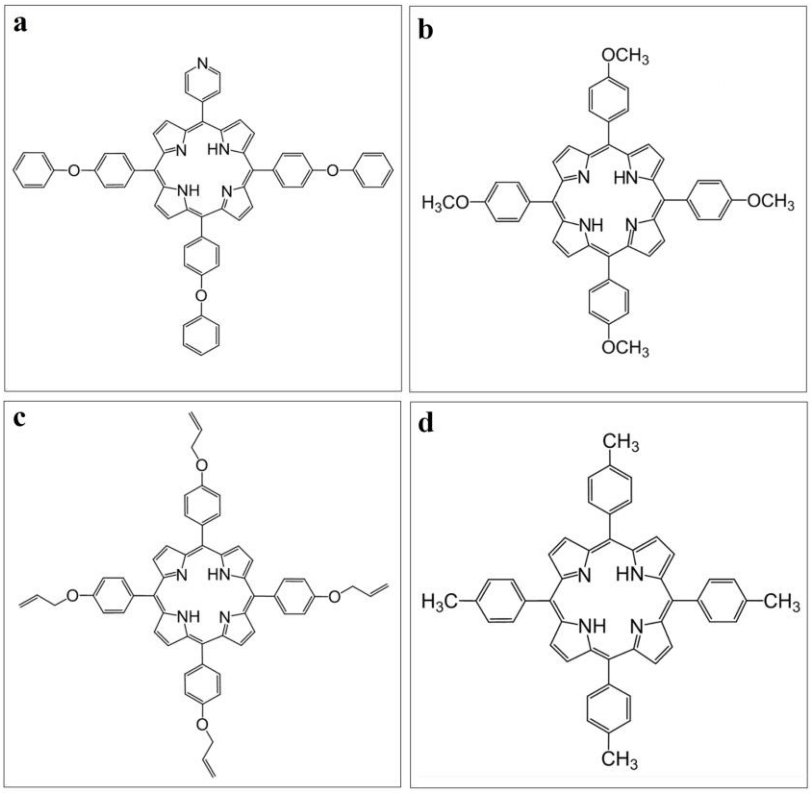

Scheme S1. The chemical structures of: a) 5-(4-pyridyl)-10,15,20-tris(4-phenoxyphenyl)porphyrin; b) 5,10,15,20-tetrakis(4-methoxyphenyl)porphyrin; c) 5,10,15,20-tetrakis(4-allyloxyphenyl)-porphyrin and d) 5,10,15,20-tetrakis(p-tolyl)porphyrin.

Equations

The electrochemical potential values measured versus the Ag/AgCl(sat. KCl) reference electrode were expressed versus the Reversible Hydrogen Electrode (RHE) using Equation (1). Equations (2) and (3) were employed to calculate the OER and HER overpotential values, while Equation (4) was applied to determine the Tafel slope [1,2].

$$E_{RHE} = E_{Ag/AgCl(sat.\ KCl)} + 0.059 \times pH + 0.197 \quad (1)$$

$$\eta_{O2} = E_{RHE} - 1.23 \quad (2)$$

$$\eta_{H2} = |E_{RHE}| \quad (3)$$

$$\eta = b \times \log(i) + a \quad (4)$$

Where: E_{RHE} is the reversible hydrogen electrode potential [V], $E_{Ag/AgCl(sat.\ KCl)}$ is the potential *vs.* the Ag/AgCl (sat. KCl) reference electrode [V], η_{O2} is the oxygen evolution overpotential and η_{H2} is the hydrogen evolution overpotential [V], η is either the oxygen or the hydrogen evolution overpotential [V], i is the current density [mA/cm^2] and b is the Tafel slope.

The classical ferrocyanide/ferricyanide redox system and the Randles-Sevcik equation - Equation (5) - were used to estimate the electroactive surface area (EASA) and the diffusion coefficient of the electroactive species for the porphyrin modified graphite electrodes that showed the highest electrocatalytic performance in the water splitting tests [3].

$$I_p = (2.69 \times 10^5) \times n^{3/2} \times A \times D^{1/2} \times C \times v^{1/2} \quad (5)$$

Where: I_p = the peak current [A]; n = the number of electrons involved in the redox process at T = 298 K; A = the surface area of the working electrode [cm^2]; D = the diffusion coefficient of the electroactive species [cm^2/s]; C = the bulk concentration of the electroactive species [M] and v = the scan rate [V/s].

For the employed redox system n = 1 and the theoretical value for the diffusion coefficient found in the literature is 6.7 x 10^{-6} cm^2/s [3,4].

Figures

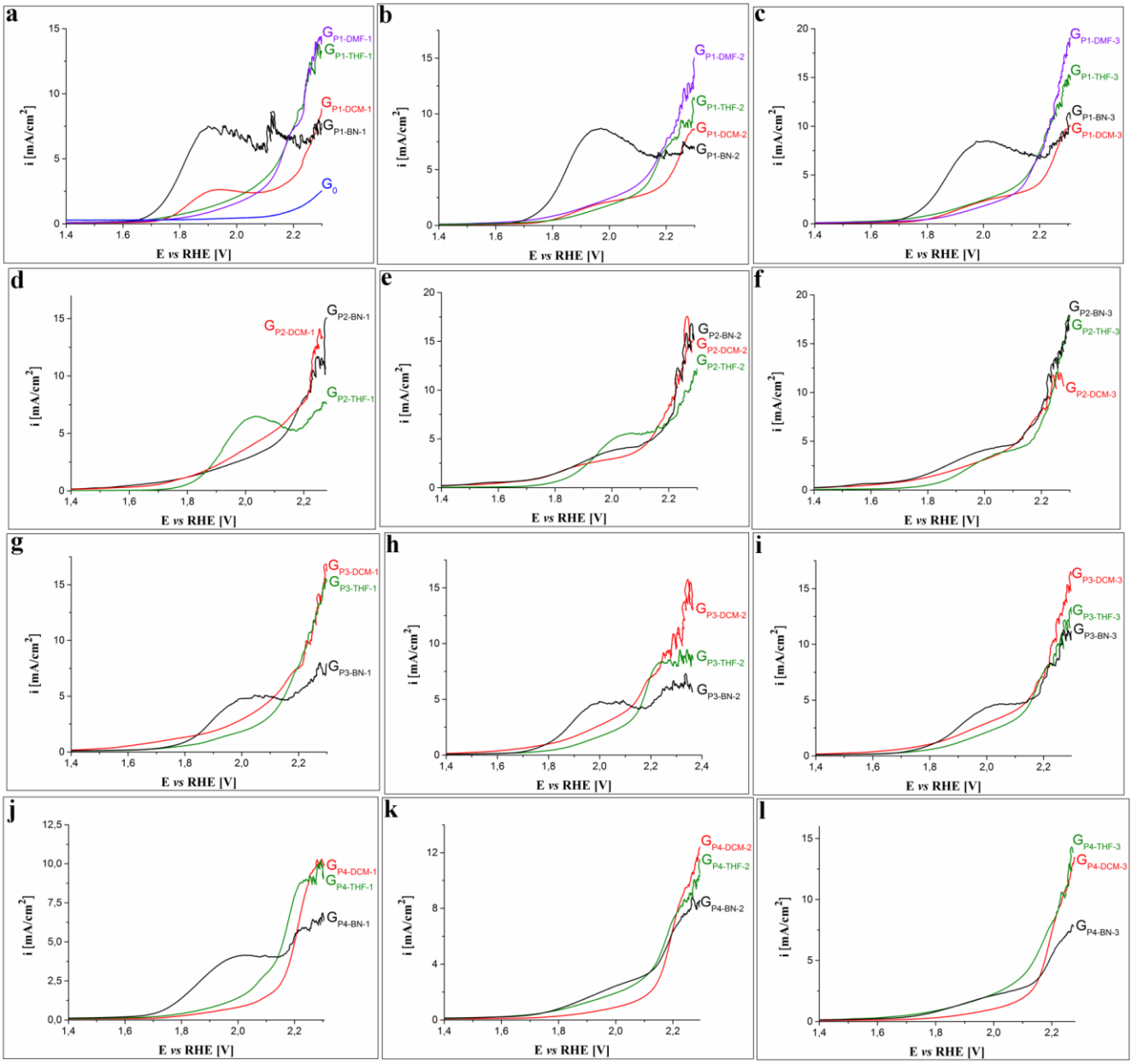

Figure S1. Anodic polarization curves recorded on the porphyrin modified graphite electrodes in 0.1M KOH solution, at v = 1 mV/s. The electrode codes are the ones specified in Table 1, and G_0 (from Figure S1a) is the unmodified graphite electrode.

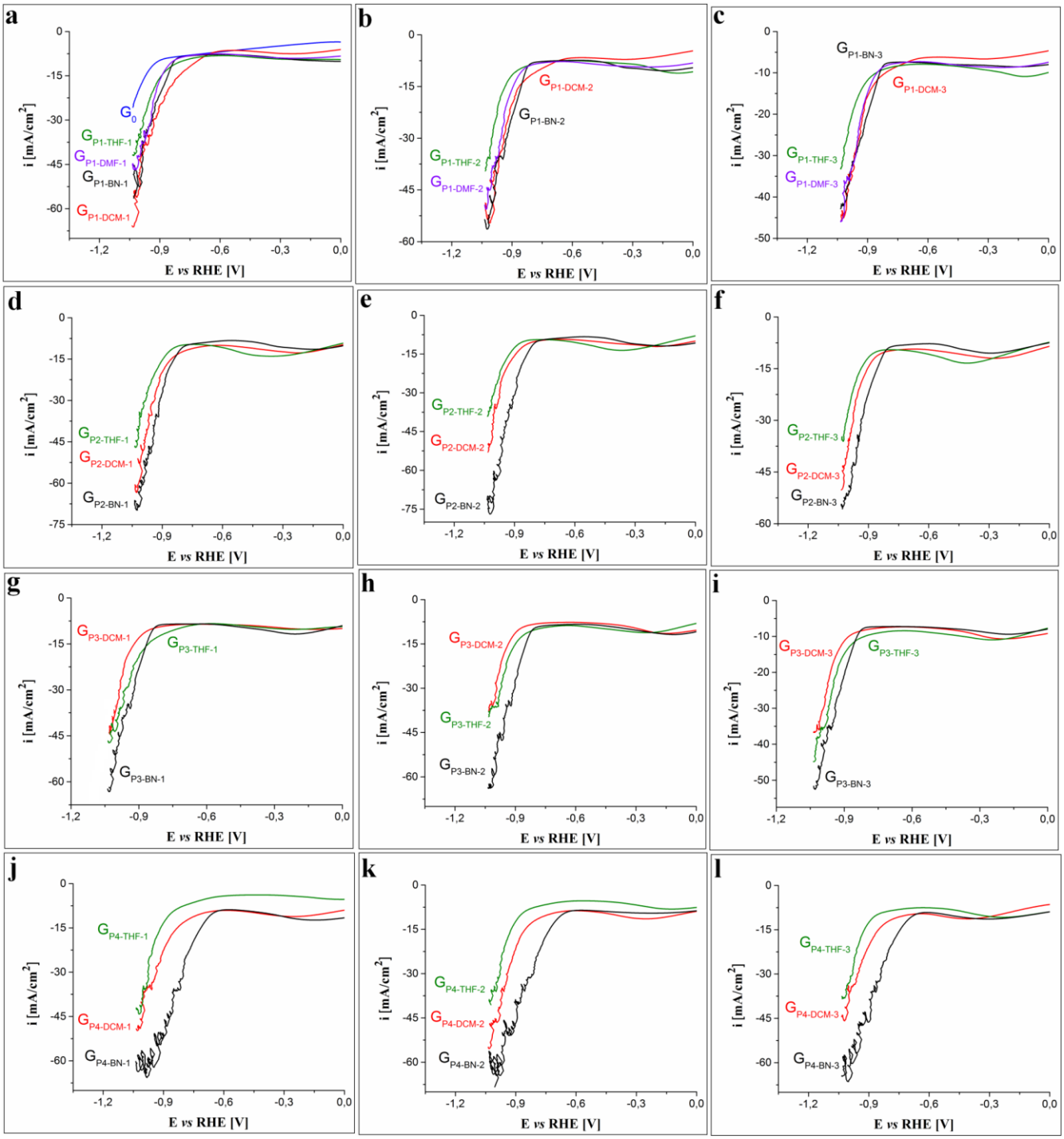

Figure S2. Cathodic polarization curves traced on the porphyrin modified graphite electrodes in 0.1M KOH solution, at v = 5 mV/s. The electrode codes are the ones specified in Table 1, and G_0 (from Figure S2a) is the unmodified graphite electrode.

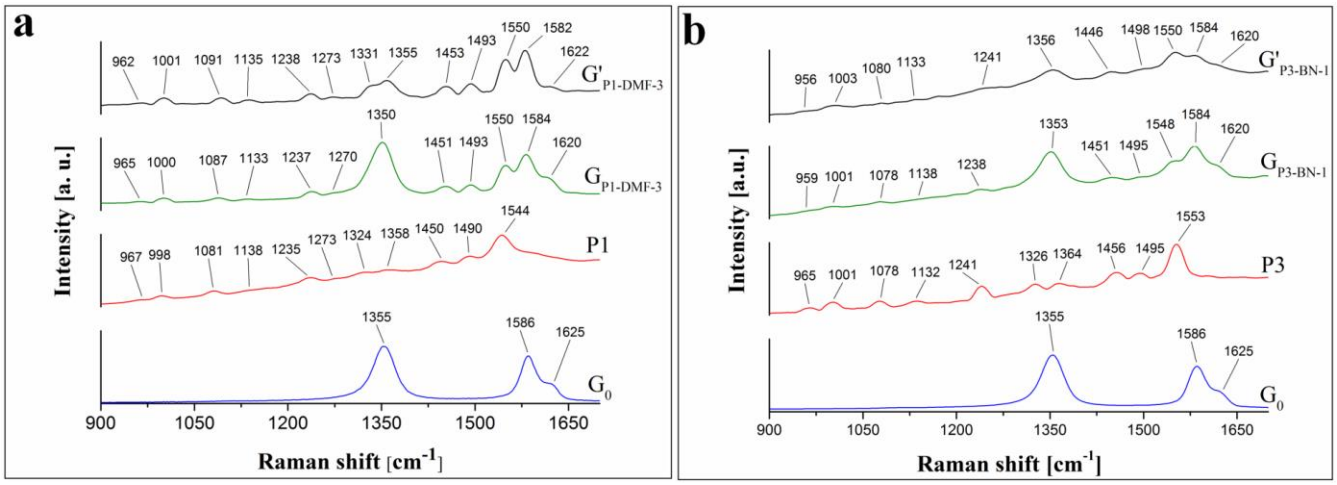

Figure S3. Raman spectra recorded on: a) G_0, P1 and the $G_{P1\text{-}DMF\text{-}3}$ electrode before and after the chronoamperometric test ($G_{P1\text{-}DMF\text{-}3}$ and $G'_{P1\text{-}DMF\text{-}3}$, respectively); b) G_0, P3 and the $G_{P3\text{-}BN\text{-}1}$ electrode before and after the chronoamperometric test ($G_{P3\text{-}BN\text{-}1}$ and $G'_{P3\text{-}BN\text{-}1}$, respectively).

References

[1] Z. Zhao, H. Wu, H. He, X. Xu, Y. Jin, Self-standing non-noble metal (Ni-Fe) oxide nanotube array anode catalysts with synergistic reactivity for high-performance water oxidation, J. Mater. Chem. A. 3 (2015) 7179–7186.

[2] B.O. Taranu, M.G. Ivanovici, P. Svera, P. Vlazan, P. Sfirloaga, M. Poienar, $Ni_{11}{\square}(HPO_3)_8(OH)_6$ multifunctional materials: Electrodes for oxygen evolution reaction and potential visible-light active photocatalysts, J. Alloys Compd. 848 (2020) 156595.

[3] S. Motoc, F. Manea, C. Orha, A. Pop, Enhanced electrochemical response of diclofenac at a fullerene–carbon nanofiber paste electrode, Sensors (Switzerland) 19 (2019) 1332.

[4] M. Yang, Y. Yang, Y. Liu, G. Shen, R. Yu, Platinum nanoparticles-doped sol-gel/carbon nanotubes composite electrochemical sensors and biosensors, Biosens. Bioelectron. 21 (2006) 1125–1131.